

Petrogenesis of xenolith-bearing basalts from southeastern Arizona

STANLEY H. EVANS, JR. AND W. P. NASH

*Department of Geology and Geophysics, University of Utah
Salt Lake City, Utah 84112*

Abstract

The Geronimo lavas consist of Quaternary alkali-olivine basalt and basanite which have been erupted over 850 km² in the San Bernardino valley, southeastern Arizona. The lava field contains flows, cones of cinder and agglutinate, and several large maars up to 1 km in diameter with associated tuff rings. The lavas contain plagioclase, titaniferous clinopyroxene, olivine, titanomagnetite, and rare spinel, ilmenite, and nepheline. Xenoliths in lavas and tuffs include lherzolite, websterite, gabbro, clinopyroxenite, and a phlogopite-bearing kaersutite peridotite. Megacrysts of olivine, clinopyroxene, kaersutite, potash oligoclase, and spinel occur in abundance. The lavas exhibit considerable chemical diversity and contain more alumina and alkalis than typical alkali-olivine basalts; some varieties contain up to 6.5 percent Na₂O and 3.4 percent K₂O. Barium (600–900 ppm) and strontium (700–1100 ppm) concentrations are substantial.

Thermodynamic calculations for equilibrium between a basanite melt and lherzolite residual material, using melt components of Al₂O₃, SiO₂, NaAlSi₃O₈, Fe₂SiO₄, and CaMgSi₂O₆, yield a solution of 1400°C and 30 kbar, equivalent to a depth of 96 km. A megacryst assemblage gives a solution of 1290°C and 13 kbar (42 km), and a phenocryst assemblage gives a solution of 1100°C and 5 kbar (16 km). The lavas could be generated by 10 percent partial melting of pyrolite, whereas lherzolite requires unrealistically small degrees of partial melting (<0.5 percent). The fractionation of high-pressure megacrysts, and phenocrysts at lower pressures, enables the derivation of all analyzed lavas from a single primary basanitic magma.

Introduction

The San Bernardino valley, southeastern Arizona, contains lavas of alkali-olivine basalts and basanites covering an area of 850 km² (Fig. 1). Volcanism over a period of 3.2 to 0.2 m.y. B.P. (Lynch, 1976) has produced extensive flows, maars, tuff rings, and approximately 130 vents and cinder cones. The vents are aligned along a NNE trend which cuts across the dominant north-south Basin and Range tectonic trend of the area.

The San Bernardino Valley is within the southern Basin and Range province, and information on the nature of the mantle beneath this portion of the province is sparse. Present geophysical data (Roy *et al.*, 1972; Langston and Helmberger, 1974) are insufficient to establish the presence of a low-velocity zone. However, the available information is similar to that on the rest of the Basin and Range province, which contains anomalous mantle material whose properties are consistent with the presence of areas of partial melting within a low-velocity zone.

The earliest volcanic activity produced basalt flows that filled the valley floor. Some of the oldest flows lie above the present valley floor along its margins and were apparently erupted prior to down-faulting of the valley. Phreatic, maar-forming eruptions cut through the valley-floor basalts. Five tuff rings are present, two of which have extensive maar craters in whose walls are exposed sequential basalt flows. Fragments of basalt, lherzolite, alkali gabbro, websterite, and kaersutite peridotite occur in the tuff rings. The most recent activity consisted of the formation of cones of agglutinate and cinder with associated lava flows. Lherzolite xenoliths are abundant in many of the lavas, whereas pyroxenite occurs much less frequently. Bombs in cinder cones are often cored with lherzolite fragments, and megacrysts of spinel, potash oligoclase, kaersutite, clinopyroxene, and olivine occur in the talus of cinder cones and in the lavas. The volcanic features of this area have been described by Lynch (1972), who referred to the area as the "Bernardino Volcanic Field". A brief description of lavas, xenoliths, and megacrysts is given by Arculus *et al.*

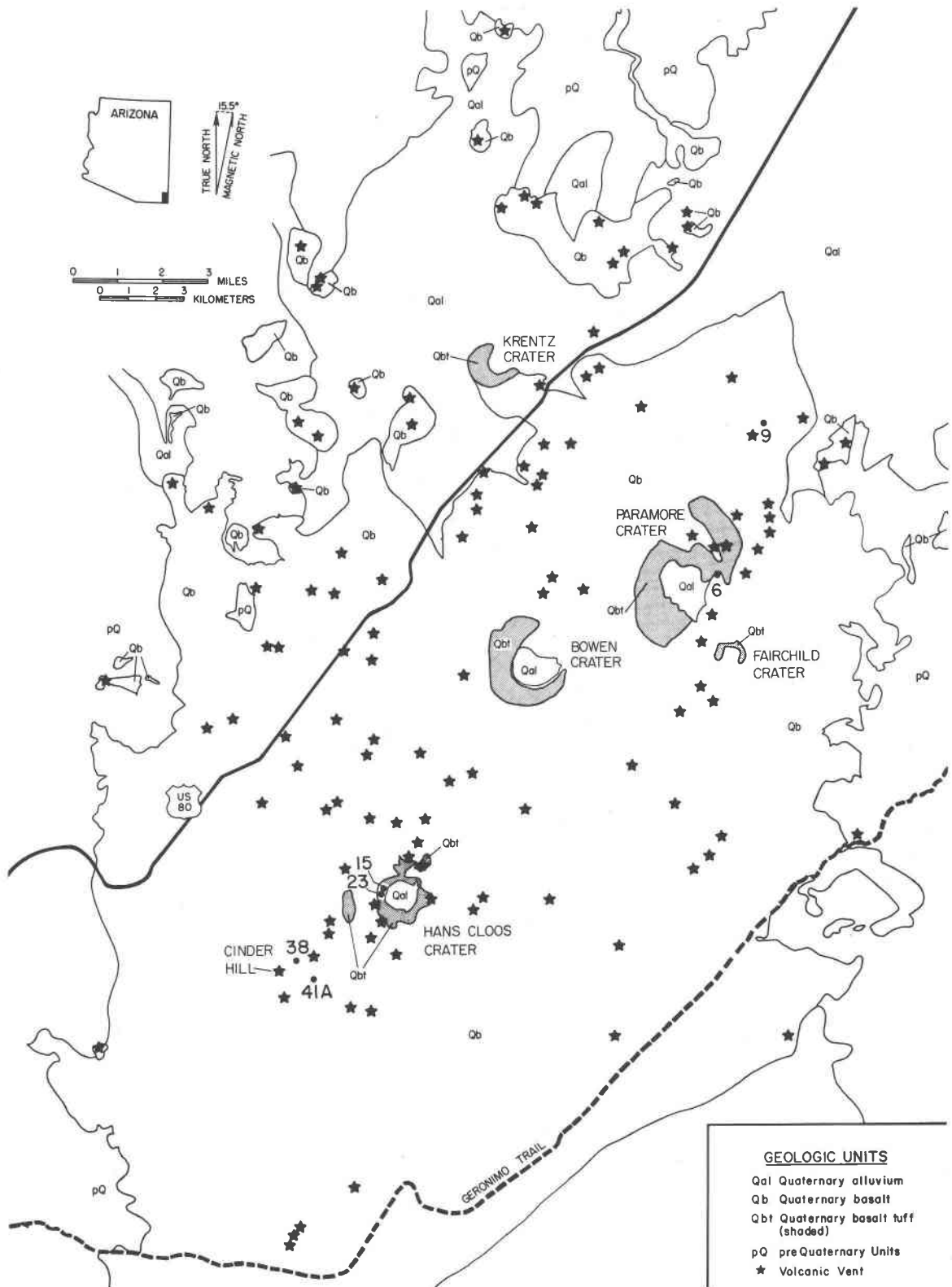


Fig. 1. Generalized geologic map of San Bernardino valley, Arizona, with locations of analyzed samples (after Lynch, 1972).

(1977), who call the lavas the Geronimo Basalts, after the last of the Apache warrior chiefs, who surrendered in this desolate valley in 1886.

Petrography

The lavas of the Geronimo volcanic field show little petrographic variation, with most due to differing degrees of crystallinity and extent of weathering. The lavas are mildly porphyritic and hypocrystalline, although some of the less crystalline varieties are not obviously porphyritic. Modes of analyzed rocks are given in Table 1. The glass content of the basalts is variable, ranging up to 50 percent. Sample 76-38, a basalt bomb from Cinder Hill, contains phenocrysts of strongly zoned euhedral clinopyroxene 0.5mm to 1.5mm long and rounded grains of deep-green aluminous spinel. It also contains phenocrysts of euhedral olivine, 0.5mm long, and rare plagioclase laths, 0.5mm long. The groundmass is a vesicular mat of plagioclase laths and titanite set in glass dusted with titanomagnetite and apatite.

Basalts from flows (samples 76-6, 9, 15, 23 and 41A) are similar to one another, usually containing megacrysts up to 2cm across of clinopyroxene as well as anhedral olivine up to 6mm across, both of which exhibit mosaic extinction. The phenocryst assemblage consists of euhedral to subhedral olivine up to 3mm in diameter which is occasionally corroded, rare anhedral orthopyroxene up to 1.5mm across surrounded by a reaction rim of olivine, and rounded grains up to 1mm across of aluminous (deep green) spinel frequently surrounded by a reaction rim of iron-titanium oxides. Phenocrysts of plagioclase are uncommon, occurring only in two lavas (76-23 and 76-41A). Typically the plagioclase occurs in small subhedral laths ranging from less than 0.05mm up to 0.5mm long. Megacrysts and phenocrysts are set in a groundmass of subhedral plagioclase laths, anhedral titanite, subhedral olivine, and euhedral titanomagnetite along with varying amounts of brown glass. In one lava (76-9) rare euhedral ilmenite needles occur in the groundmass. In sample 76-15 the

Table 1. Modal analyses of Geronimo basalts (volume percent)

Rock	Plagioclase	Clinopyroxene	Orthopyroxene	Olivine	Spinel	Amphibole	Phlogopite	Oxide	Groundmass
76-6	10.5	5.7	-	9.0	-	-	-	3.0	71.8
76-9	0.5	0.8	-	6.3	-	-	-	0.4	92.0
76-15	1.5	3.1	-	5.9	-	-	-	1.2	88.3
76-23	9.6	10.7	-	12.0	0.3	-	-	2.4	65.0
76-38	1.0	5.7	-	9.3	0.6	-	-	3.5	79.9
76-41A	23.5	33.2	-	10.2	0.1	-	-	4.6	28.4
HC76-2	50.4	36.9	2.4	-	4.2	-	-	-	6.1
HC76-4	-	54.0	40.6	-	0.4	-	-	-	-
HC76-7	-	76.1	-	7.8	9.7	-	-	-	6.4
PC76-2	1.6	55.0	-	4.1	1.1	31.5	0.1	-	6.6
PC76-6	-	11.9	17.1	67.5	2.8	-	-	-	0.7

Key to Sample Localities

Sample #	Rock Type and Localities
76-6	Basalt Flow, Paramore Crater
76-9	Basalt Flow, N. E. of Paramore Crater
76-15	Basalt Flow, Hans Cloos Crater
76-23	Basalt Flow, Hans Cloos Crater
76-38	Basalt Bomb, Cinder Hill
76-41A	Basalt Flow, Cinder Hill
HC76-2	Alkali Gabbro, Hans Cloos Crater
HC76-4	Websterite, Hans Cloos Crater
HC76-7	Clinopyroxenite, Hans Cloos Crater
PC76-2	Kaersutite Peridotite, Paramore Crater
PC76-6	Lherzolite, Paramore Crater

presence of groundmass nepheline was suspected and was subsequently confirmed by X-ray diffraction.

Five representative samples of xenoliths were selected for analysis; modes are given in Table 1. All xenoliths except spinel lherzolite are of the variety termed type II by Frey and Prinz (1978) in their study of ultramafic inclusions in basanite from San Carlos, Arizona. This class of inclusion is characterized by pyroxenes with relatively high titanium and low chromium contents, together with a relatively lower $MgO/(FeO + MgO)$ ratio. Spinel from Group II are green, rich in aluminum and poor in chromium. Typically, Group II inclusions have been interpreted as cognate inclusions. Alkali gabbro xenoliths (sample HC76-2) are rare and are composed chiefly of anhedral, 5–6mm plagioclase which poikilitically encloses embayed and corroded clinopyroxene. The plagioclase shows indications of deformation such as kink banding, undulatory extinction and mylonitization along grain margins. In thin section the clinopyroxene is lilac-brown, and isolated grains enclosed in plagioclase are optically continuous. Clinopyroxene contains abundant exsolution lamellae of orthopyroxene as well as irregular blebs extending out from lamellae, and most clinopyroxene shows mosaic extinction. Spinel is abundant in this type of xenolith, occurring as anhedral blebs in plagioclase and occasionally in clinopyroxene. In hand specimen the xenolith displays obvious banding, with alternating feldspar- and pyroxene-rich layers. The texture is quite similar to mafic granulites described by Wilkinson (1975). The compositional banding is consistent with a cumulate origin. If this is so, pyroxene is the cumulus phase, plagioclase is intercumulus, and post-cumulus growth of plagioclase has taken place at the expense of pyroxene.

Websterite (sample HC76-4) is composed of nearly equal amounts of clinopyroxene and orthopyroxene. These minerals occur in a polygonal aggregate with anhedral ortho- and clinopyroxene of equal size, 1–3mm. Kink bands and undulatory extinction are common in both pyroxenes, and rare lamellae of orthopyroxene are present in clinopyroxene. These lamellae are confined to the interior of the grains and die out near grain margins. Small anhedral spinels less than 0.5mm in diameter occur at grain junctions of the pyroxenes. The texture of this rock is virtually identical to that illustrated by Wilkinson (1975, Fig. 2).

In clinopyroxenite xenoliths (sample HC76-7) abundant anhedral brown clinopyroxene encloses subhedral blue-green spinel. The equigranular clinopyroxene grains are 1.3 to 1.4cm across. Spinel occurs interstitially as well as poikilitically enclosed in pyroxene. The pyroxene is strained, showing both undulatory and mosaic extinction similar to pyroxene in sample HC76-2.

In kaersutite peridotite xenoliths (sample PC76-2) large (4–5mm) grains of kaersutite poikilitically enclose clinopyroxene. Clinopyroxene occurs also as anhedral grains 1mm across. The separate areas of anhedral clinopyroxene, not enclosed in kaersutite, seem to have no reaction relation with kaersutite even when they share common grain boundaries. In contrast, clinopyroxene enclosed in kaersutite contains broad lamellae of kaersutite; apparently the clinopyroxene is being replaced by kaersutite. Olivine, anhedral and 1–1.5mm in diameter, is also present. It is equigranular and shows no reaction relationship with kaersutite. Blue-green aluminous spinel less than 0.05mm across occurs as rounded grains in olivine and as irregular interstitial masses associated with kaersutite. Both plagioclase and phlogopite occur as minor interstitial phases in both kaersutite-rich and pyroxene-rich areas, and pyrrhotite is present as small isolated grains in kaersutite. This xenolith appears to have a complex origin, and bears a striking resemblance to kaersutite inclusions described by Best (1970, 1975). The presence of exsolution lamellae, and undulatory and mosaic extinction in plagioclase and pyroxene, suggest this xenolith is of metamorphic origin. Alternatively, the xenolith may be a cumulate with clinopyroxene as the cumulus phase and kaersutite representing an inter-cumulate liquid, along with plagioclase and phlogopite. If so, post-cumulus replacement of clinopyroxene is shown by wide lamellae of kaersutite in the clinopyroxene.

The most abundant xenolith type in the Geronimo

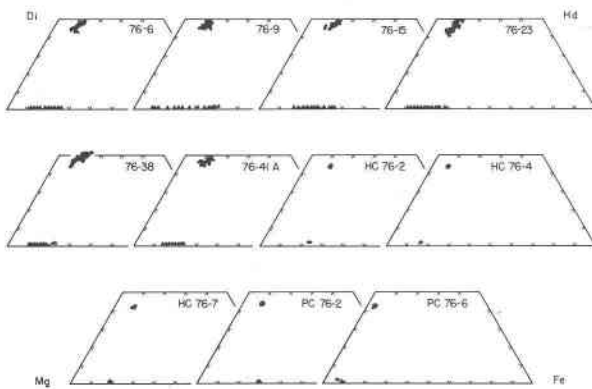


Fig. 2. Microprobe analyses of pyroxene and olivine of Geronimo basalts in atom percent Ca, Fe, Mg. Filled circles, pyroxene; filled triangles, olivine.

basalts is lherzolite (sample PC76-6), which occurs in tuffs and lavas as well as in cores of bombs in cinder cones. The lherzolites consist of a polygonal aggregate of anhedral olivine 2.5–3mm across with minor kink-banding, anhedral laths of orthopyroxene 1–4mm long typically with undulatory extinction, anhedral green chrome diopside 1mm in diameter, and brown chromian spinel interstitial to the other phases. No segregation or banding of minerals is apparent in the lherzolites either in thin section or at hand-specimen scale.

Mineralogy

Mineral analyses were done on an ARL-EMX-SM electron microprobe using mineral standards and employing standard correction techniques when appropriate (Bence and Albee, 1968; Albee and Ray, 1970).

Olivine

Two varieties of olivine occur in the Geronimo basalts. The first are rounded, anhedral grains (1–2mm) showing evidence of strain such as mosaic extinction. The other type of olivine is euhedral to subhedral (0.05 to 0.5mm) and is a groundmass phase. Figure 2 shows the range in composition for

groundmass olivines. The extreme range encountered is from Fo₉₀ to Fo₆₀ for lavas 76-6 and 76-9. The most restricted range is in lava 76-38 (Fo₉₀ to Fo₇₇), which probably had a more limited crystallization interval than the other basalts. There is a detectable variation in the calcium of individual groundmass olivines from 0.19 to 0.48 percent CaO, which could be consistent with a lowering of pressure as crystallization of olivine progressed (Stormer, 1973), or it could be a kinetic effect similar to that described by Donaldson *et al.* (1975), who demonstrated that calcium contents of synthetic olivines vary with cooling rates. Average compositions for groundmass olivines are presented in Table 2.

Olivine occurs in three types of xenoliths. In clinopyroxenite (sample HC76-7) olivine is a minor phase of nearly constant composition, zoned from cores of Fo₈₄ to rims of Fo₈₀ (Fig. 2). Olivine is also present in kaersutite peridotite (sample PC76-2) but again is a minor phase and is essentially unzoned. Olivine in lherzolite (sample PC76-6) is unzoned and contains little calcium, indicating high-pressure crystallization. Olivines in lherzolite contain two to ten times as much NiO as those from other rock types. An analysis of an olivine megacryst is presented in

Table 2. Average microprobe analyses and structural formulas of olivines

	76 -6	76 -9	76 -15	76 -23	76 -38	76 -41A	HC76 -7	PC76 -2	PC76 -6	76 -35
SiO ₂	38.6	39.2	36.9	39.0	39.3	38.3	38.2	37.0	40.5	40.0
FeO	20.5	19.1	25.0	19.4	15.9	19.6	19.6	27.1	10.1	12.3
MnO	0.26	0.11	0.48	0.47	0.15	0.17	0.18	0.30	0.04	0.16
MgO	40.4	40.9	37.1	41.7	44.0	42.0	41.6	34.3	48.4	46.9
CaO	0.43	0.51	0.43	0.19	0.48	0.46	0.33	0.29	0.20	0.20
NiO	0.04	0.03	0.01	0.00	0.02	0.01	0.00	0.00	0.12	0.10
Total	100.2	99.9	99.9	100.8	99.9	100.5	99.9	99.0	99.4	99.7
Number of Atoms Based on 4 Oxygens										
Si	0.99	1.01	0.98	0.99	0.99	0.98	0.98	1.00	1.00	0.99
Fe	0.44	0.41	0.55	0.41	0.34	0.42	0.42	0.61	0.21	0.26
Mn	0.01	0.00	0.01	0.01	0.00	0.01	0.01	0.01	0.00	0.00
Mg	1.55	1.56	1.47	1.58	1.66	1.60	1.60	1.37	1.78	1.74
Ca	0.01	0.01	0.01	0.01	0.01	0.01	0.01	0.01	0.01	0.01
Ni	0.00	0.00	0.00	0.00	0.00	0.00	0.00	0.00	0.00	0.00
Weight %										
Fo	70.5	71.4	54.7	72.8	76.8	73.3	72.6	59.9	84.5	81.8
Fa	29.1	27.1	35.5	27.5	22.6	27.8	27.8	38.4	14.3	17.4
La	0.66	0.78	0.66	0.29	0.74	0.71	0.51	0.45	0.31	0.31
Total	100.3	99.3	100.9	100.6	100.1	101.8	100.9	98.8	99.1	99.5
Mole %										
Fo	0.77	0.79	0.69	0.79	0.83	0.78	0.78	0.69	0.89	0.87
Fa	0.23	0.21	0.31	0.21	0.17	0.22	0.22	0.31	0.11	0.13

Table 2 (SBV76-35). This olivine is similar to those in lherzolite, but the grain was much larger (approximately 2cm) than any observed in lherzolites.

Pyroxene

Phenocrysts of pyroxene are rare. A few scattered megacrysts occur, but are normally zoned and are surrounded by reaction rims of olivine. The groundmass pyroxene is calcic augite. It is abundant in the groundmass and consists of small anhedral grains intergrown with feldspar. In Figure 2 augite has an apparent trend towards the Di-Hd join. This trend appears because the pyroxenes do not lie in the plane of projection; this is typical of silica-undersaturated lavas. It reflects the greater substitution of Al for Si in the Y site, causing a sympathetic decrease in Mg and Fe and an increase in the Ca/(Fe + Mg) ratio as pyroxenes become more enriched in Ti and Al endmembers. Figure 2 presents analyses of groundmass pyroxenes for the lavas, and Table 3 contains average analyses for the pyroxenes. Clinopyroxene phenocrysts commonly have a sieve-texture core surrounded by an inclusion-free rim. This texture, among several, has been attributed to rapid crystalli-

zation under supercooled conditions (Lofgren *et al.*, 1974, 1975; Donaldson *et al.*, 1975; Gutmann, 1977). Assumptions of equilibrium between phenocrysts and magmas made subsequently in this paper would not be valid if phenocryst compositions were affected by kinetic phenomena. No skeletal, dendritic, spherulitic, or acicular textures were observed in any phenocryst phases, nor do phenocrysts of olivine and plagioclase have sieve textures. Similarly, none of these textural features was found in the megacryst assemblage.

Both clinopyroxene and orthopyroxene occur in many of the xenoliths. Average analyses of coexisting clino- and orthopyroxene (for samples HC76-2 and HC76-4) are presented in Table 3. For sample HC76-7 average analyses of both the clinopyroxene host and orthopyroxene lamellae are given. Figure 2 shows that pyroxenes are quite uniform in composition in all xenoliths. Clinopyroxenes are nearly all aluminous diopsides and orthopyroxenes are aluminous bronzites, except in the lherzolite where the orthopyroxene is aluminous enstatite. An analysis of a clinopyroxene megacryst from Hans Cloos maar is also given in Table 3.

Table 3. Average microprobe analyses and structural formulas of pyroxenes

	76-6 (Cpx)	76-9 (Cpx)	76-15 (Cpx)	76-23 (Cpx)	76-38 (Cpx)	76-41 (Cpx)	HC76-2 (Cpx)	HC76-2 (Opx)
SiO ₂	48.4	47.2	46.6	45.3	46.0	44.5	50.2	51.4
TiO ₂	1.82	2.64	2.76	3.27	2.93	3.84	0.85	0.41
Al ₂ O ₃	6.94	7.31	7.66	9.03	7.52	7.92	7.85	5.70
Cr ₂ O ₃	0.06	0.08	0.02	0.25	0.19	0.02	0.02	0.06
FeO	7.48	8.35	8.35	7.40	7.74	8.14	7.42	16.6
MnO	0.24	0.20	0.21	0.13	0.14	0.19	0.20	0.23
MgO	12.1	11.2	11.0	12.1	11.4	11.8	12.5	23.5
CaO	22.0	22.8	23.2	22.6	23.1	22.9	20.3	1.50
Na ₂ O	0.78	0.65	0.68	0.61	0.50	0.64	0.96	0.13
Total	99.8	100.4	100.5	100.7	99.5	100.0	100.3	99.5
Number of Atoms Based on 6 Oxygens								
Si ^{IV}	1.81	1.77	1.75	1.69	1.74	1.68	1.85	1.88
Al ^{IV}	0.19	0.23	0.25	0.31	0.26	0.32	0.15	0.12
Al ^{VI}	0.12	0.09	0.09	0.09	0.08	0.03	0.19	0.13
Ti	0.05	0.07	0.08	0.09	0.08	0.11	0.02	0.01
Cr	-	-	-	-	-	-	-	-
Fe	0.23	0.26	0.26	0.23	0.24	0.26	0.23	0.51
Mn	0.01	0.01	0.01			0.01	0.01	0.01
Mg	0.67	0.62	0.61	0.67	0.64	0.67	0.69	1.28
Ca	0.88	0.92	0.93	0.90	0.94	0.93	0.80	0.06
Na	0.06	0.05	0.04	0.04	0.04	0.04	0.07	0.01

Feldspar

Plagioclase phenocrysts occur in two lavas (76-23 and 76-41A). They range in composition from cores of $An_{67}Ab_{30}Or_3$ to rims of $An_{48}Ab_{47}Or_5$. Feldspar analyses are shown in Figure 3. Groundmass compositions range from $An_{75}Ab_{23}Or_2$ to compositions approaching sanidine. Plagioclase is extremely abundant, whereas alkali feldspar is rare and occurs as interstitial masses difficult to analyze.

Plagioclase is present in two xenoliths. In gabbro (HC76-2) plagioclase is restricted in zoning from cores of $An_{65}Ab_{34}Or_1$ to rims of $An_{53}Ab_{45}Or_2$. Interstitial plagioclase in kaersutite peridotite (PC76-2) ranges from $An_{50}Ab_{48}Or_2$ to $An_{45}Ab_{53}Or_2$.

Three megacrysts were analyzed, and their compositions are also shown in Figure 3. The feldspars are essentially unzoned; megacrysts from Hans Cloos crater and Paramore crater are identical, whereas feldspar from Cinder Hill is slightly more calcic and less potassic. These megacrysts are similar to those described from other localities. Binns *et al.* (1970) described a suite of megacrysts from northeastern New South Wales, Australia, containing anortho-

class, which is lower in anorthite and richer in orthoclase than the oligoclases from the Geronimo basalts. Their megacryst suite also contains more An-rich varieties of plagioclase than are encountered in the Geronimo basalts. Hoffer and Hoffer (1973) described feldspar megacrysts from the Potrillo basalt, New Mexico, which, like the Australian megacrysts, display a wider compositional range.

Although potash oligoclase has not been encountered in melting experiments on basanitic compositions, its common presence in nature suggests that it is a stable phase in such liquids. Moreover, thermochemical arguments (Bacon and Carmichael, 1973) indicate that sodic plagioclase is the feldspar to be expected in mafic alkalic magmas under conditions approximating the crust-mantle boundary.

Kaersutite and phlogopite

Kaersutite (Table 4) occurs both as the major constituent of xenolith PC76-2 and as megacrysts. The kaersutites are comparable in composition to those from the Grand Canyon area (Best, 1970, 1975) and the Lake Turkana region of Africa (Brown and Carmichael, 1969), but are more titaniferous and lower

Table 3. (continued)

	HC76-4 (Cpx)	HC76-4 (Opx)	HC76-7 (Cpx)	HC76-7 (Opx)	PC76-2 (Cpx)	PC76-6 (Cpx)	PC76-6 (Opx)	Hans Cloos (Cpx)
SiO ₂	49.4	51.3	48.2	50.6	51.4	51.4	53.5	48.9
TiO ₂	0.70	0.18	1.39	0.32	0.56	0.39	0.10	0.63
Al ₂ O ₃	8.45	5.75	9.10	6.83	5.48	6.66	4.22	8.87
Cr ₂ O ₃	0.10	0.06	0.01	0.01	0.10	0.70	0.33	0.44
FeO	5.35	12.5	6.58	11.8	6.79	2.90	6.34	5.16
MnO	0.15	0.23	0.16	0.25	0.17	0.08	0.12	0.14
MgO	13.6	28.3	13.7	27.8	13.9	16.0	34.0	16.7
CaO	21.7	1.13	20.2	1.77	21.1	20.9	0.87	18.2
Na ₂ O	0.90	0.05	0.99	0.16	0.95	1.38	0.10	1.04
Total	100.4	99.5	100.3	99.5	100.5	100.4	99.6	100.1
Number of Atoms Based on 6 Oxygens								
Si ^{IV}	1.81	1.84	1.77	1.81	1.89	1.86	1.87	1.78
Al ^{IV}	0.19	0.16	0.23	0.19	0.11	0.14	0.13	0.22
Al ^{VI}	0.18	0.08	0.15	0.10	0.13	0.14	0.04	0.16
Ti	0.02	0.01	0.04	0.01	0.01	0.01	-	0.02
Cr	-	-	-	-	-	0.02	0.01	0.01
Fe	0.16	0.38	0.20	0.35	0.21	0.09	0.18	0.16
Mn	0.01	0.01	0.01	0.01	0.01	0.01	-	-
Mg	0.74	1.51	0.75	1.49	0.76	0.86	1.77	0.91
Ca	0.85	0.04	0.80	0.07	0.83	0.81	0.03	0.71
Na	0.06	-	0.07	0.01	0.06	0.10	0.01	0.08

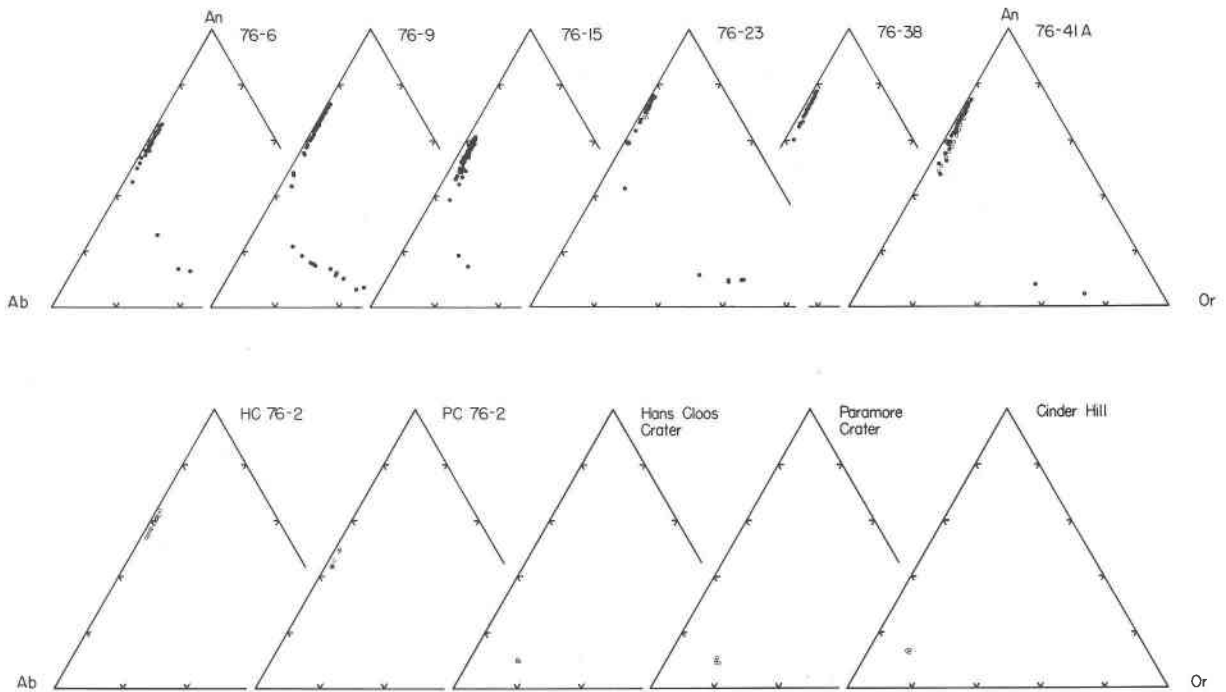


Fig. 3. Microprobe analyses of feldspars of Geronimo basalts in mole percent anorthite (An), albite (Ab), and orthoclase (Or). Filled circles, groundmass compositions; open circles, phenocryst and megacryst compositions.

in MgO than kaersutites described by Wilkinson (1975) from Australia.

Phlogopite is present interstitially in kaersutite peridotite; an average analysis is given in Table 4. It contains substantial BaO and TiO₂ and measurable amounts of Cl and F. Two analyses of phlogopite from peridotite inclusions from Australia (Frey and Green, 1974) have substantially more MgO and less FeO than this phlogopite. Wilkinson (1975) gives two analyses of megacrysts from ultramafic inclusions in an analcinite sill in northeastern New South Wales which although containing more TiO₂ and less SiO₂ are comparable to the phlogopite described here.

Oxides

Table 5 gives analyses of ilmenite, magnetite, and spinel from lavas, xenoliths, and megacrysts. In one lava (76-9) both ilmenite and magnetite coexist in the groundmass. This pair of oxides gives an equilibration temperature of 1050°C and an oxygen fugacity of 10^{-10.4} with the thermometer-geobarometer of Buddington and Lindsley (1964). Groundmass magnetite analyses for other lavas are given in Table 5; ulvöspinel compositions vary from 59.7 to 76.1 percent.

Spinel is common as a megacryst. It is aluminous in the lavas and xenoliths, with the exception of chro-

mian spinel in lherzolite. Spinel analyses, with FeO recalculated by making $Fe^{2+} = 2Ti$, $R^{2+} = R^{3+}$ and then excess FeO allocated to equivalent magnetite, are given in Table 5. These spinels are comparable to those from Australia described by Wilkinson (1975), who also found that aluminous varieties of spinel are confined to other ultramafic inclusions, whereas chromian spinels were more common in lherzolite. Frey and Green (1974) gave analyses of chromian spinels from lherzolites which contain up to three times as much Cr₂O₃ as spinel from Geronimo lherzolite.

Accessory minerals

Apatite needles are common in the groundmass of the basalts, and pyrrhotite grains are scattered throughout kaersutite in kaersutite peridotite. The average pyrrhotite composition (weight percent) is 45.6 Fe, 50.9 S and 3.3 Ni.

Chemistry

Table 6 gives chemical analyses and CIPW norms of six lavas and five xenoliths, with an electron microprobe analysis of residual glass from the same flow as sample 76-41A. The wet-chemical methods of analysis for most elements are those of Carmichael *et al.* (1968); in addition, NiO and Cr₂O₃ were analyzed by

atomic absorption spectrophotometry. The lavas are low in silica and high in alumina and alkalis, resulting in substantial amounts of nepheline in the norm (9.7 to 23.2 percent Ne). Chemically these rocks are basanites, although the presence of modal nepheline was confirmed in only one sample (76-15). For the most part these lavas are comparable to others in the western United States, particularly those from the Rio Grande Rift. The less evolved Geronimo basalts such as 76-23, 76-38 and 76-9 are similar to those of the Bandera lava field (Laughlin *et al.*, 1972) and the Potrillo volcanics (Hoffer, 1971) east of the Geronimo field in southwestern New Mexico. The Geronimo basalts are more undersaturated than basanitic lavas in southeastern California described by Smith and Carmichael (1969) and those of the San Quintin Field, Baja California (Bacon and Carmichael, 1973).

The xenolith chemistry is rather straightforward. The alkali gabbro (HC76-2) is slightly undersaturated with respect to silica and contains appreciable normative feldspar. The websterite (HC76-4) contains normative orthopyroxene and clinopyroxene, as well as substantial anorthite reflecting the aluminous nature of the pyroxene. The clinopyroxene (HC76-7) is undersaturated and also contains substantial normative anorthite as a consequence of the high alumina content of the pyroxenes. The kaersutite (PC76-2) contains normative nepheline, with alkalis and alumina accommodated in normative feldspar in excess of its presence modally in the xenolith. The lherzolite (PC76-6) contains substantial olivine in the norm, and the norm agrees with the mode extremely well if account is taken of the presence of alumina in pyroxene rather than in feldspar.

The residual glass shows extreme enrichment in alkalis and alumina. It is peralkaline even though Al_2O_3 constitutes 21 percent of the analysis; normative nepheline and leucite are substantial.

Table 7 gives values determined by X-ray spectrometry for selected trace elements in basalts and xenoliths. Xenoliths are depleted in most incompatible elements. This is particularly true for lherzolite and websterite, which suggests that these xenoliths represent refractory mantle material from which magma has been extracted; they are not good candidates for unmodified mantle source materials.

Trace elements exhibit a systematic variation with respect to differentiation index (Thornton and Tuttle, 1960). Ba, Zr, Sr, Rb, Nb and the light rare earths are enriched in the more differentiated rocks, and some differentiation process such as crystal fractionation is strongly suggested for the Geronimo basalts.

Table 4. Average microprobe analyses and structural formulas of phlogopite and kaersutite

	PC76-2 phlogopite	PC76 -2	Hans C100s Xenocryst	Paramore Xenocryst
SiO ₂	37.6	41.3	39.7	39.9
TiO ₂	4.69	3.84	5.40	6.14
Al ₂ O ₃	16.5	14.5	14.5	14.8
FeO	10.7	9.89	13.9	12.0
MnO	0.05	0.11	0.20	0.15
MgO	16.8	13.4	9.75	11.0
CaO	0.18	11.3	10.9	10.9
BaO	0.50	0.04	0.08	0.04
Na ₂ O	0.58	2.72	2.67	2.68
K ₂ O	9.06	1.43	1.64	1.16
Rb ₂ O	0.06	-	-	-
Cl	0.02	0.03	0.02	0.01
F	0.20	0.07	0.17	0.16
Sum	97.1	98.6	98.9	93.9
-O = Cl, F	0.08	0.04	0.07	0.07
Total	97.0	98.2	98.9	98.9

	Number of Atoms Based on:			
	22 Oxygens		23 Oxygens	
Si	5.43	6.00	5.90	5.86
Al	2.57	2.00	2.10	2.14
Al	0.24	0.48	0.44	0.42
Ti	0.51	0.42	0.61	0.68
Fe	1.29	1.20	1.73	1.47
Mn	0.01	0.01	0.02	0.02
Mg	3.62	2.90	2.16	2.40
Ca	0.03	1.76	1.74	1.71
Ba	0.03	-	-	-
Na	0.19	0.86	0.76	0.76
K	1.67	0.26	0.32	0.22
OH, F	2.00	2.00	2.00	2.00

Crystal fractionation model

A model for crystal fractionation in the Geronimo basalts has been developed with an interactive computer program which solves an overdetermined set of linear mass balance equations by a least-squares method (Stormer and Nicholls, 1978). From a bulk-chemical analysis of proposed parent and daughter plus compositions of mineral phases thought to have been fractionated, one can calculate the amount of phases that must be added to or subtracted from the parent magma in order to obtain the daughter.

We have adopted basanite 76-9 as representative of the parental magma. More mafic lavas 76-23 and 76-38 appear to be cumulate (Table 1). Cinder Hill, a large Recent cinder cone from which 76-38 was collected, has erupted abundant megacrysts. Lava 76-38 can be derived from 76-9 by fractionation of these megacryst phases (Fig. 4). The process calls for the accumulation of clinopyroxene, olivine, and kaersutite, and the removal of potash oligoclase and a mi-

Table 5. Average microprobe analyses of iron-titanium oxides and spinels

	Ilmenite		Magnetites					Spinel								
	76 -9	76 -6	76 -9	76 -15	76 -23	76 -38	76 -41A	76 -6	76 -9	76 -23	76 -41A	HC76 -2	HC76 -7	PC76 -2	PC76 -6	Cinder Hill
SiO ₂	0.55	0.43	0.32	0.53	0.36	0.71	0.53	0.16	0.19	0.18	0.11	0.19	0.14	0.07	0.12	0.12
TiO ₂	48.1	24.6	24.7	21.9	25.0	21.3	27.4	0.10	0.14	0.21	0.26	0.51	0.19	0.08	0.03	0.38
Al ₂ O ₃	0.51	2.02	1.62	4.24	4.34	5.59	3.21	58.0	60.1	55.1	55.4	59.3	59.7	58.2	54.8	60.5
Cr ₂ O ₃	0.06	0.44	0.15	0.58	0.17	0.11	0.27	0.36	0.11	0.21	0.16	0.63	0.24	2.27	11.9	0.05
V ₂ O ₃	0.11	0.47	0.38	0.32	0.48	0.40	0.48	0.15	0.13	0.13	0.15	0.11	0.15	0.10	0.09	0.13
FeO	44.8	67.1	67.1	65.8	64.1	63.2	63.2	26.4	18.4	27.2	27.5	19.7	21.1	23.3	11.0	17.9
MnO	1.09	0.93	0.89	0.97	0.94	0.90	0.91	0.31	0.16	0.29	0.21	0.12	0.17	0.21	0.14	0.16
MgO	3.31	1.17	2.18	3.29	2.52	4.08	2.34	13.6	19.3	13.1	13.0	18.0	16.9	14.4	20.9	19.3
CaO	0.29	0.25	0.41	0.23	0.27	0.31	0.42	0.33	0.30	0.38	0.32	0.58	0.37	0.39	0.18	0.02
NiO	n.a.	n.a.	n.a.	n.a.	n.a.	n.a.	n.a.	0.21	0.21	0.15	0.13	0.25	0.23	0.24	0.46	0.26
ZnO	0.17	0.52	0.65	0.46	0.47	0.32	0.32	0.28	0.18	0.39	0.33	0.07	0.23	0.40	0.19	0.10
Sum	99.0	97.9	98.4	98.3	98.7	96.9	99.1	99.6	99.2	97.3	97.6	99.5	99.4	99.7	99.8	98.9
Recalc. Fe ₂ O ₃	9.35	17.6	19.5	21.7	15.6	20.7	11.8	14.3	15.4	18.8	17.3	13.9	13.9	11.6	6.8	13.5
FeO	36.4	51.3	49.5	46.2	50.0	44.6	52.6	13.2	4.5	10.3	11.9	7.2	8.6	12.9	4.9	5.8
Total	99.9	99.7	100.3	100.4	100.2	99.0	100.3	101.0	100.8	99.2	99.3	100.9	100.8	100.9	100.5	100.3
Mol % Ulvosp.		69.8	68.8	60.7	68.8	59.7	76.1									
Mol % Fe ₂ O ₃	8.7	-	-	-	-	-	-									
Temp.			1050°C	-	-	-	-									
-log f _{O₂}			10.35	-	-	-	-									

n.a. = Not analyzed.

Fe₂O₃ calculated using the method of Carmichael (1967), T and -log f_{O₂} are taken from the curves of Buddington and Lindsley (1964).

nor amount of spinel. Oligoclase could be removed by flotation; at mantle temperatures and pressures oligoclase should have a density of approximately 2.6 gm/cc, whereas the magma would have a density of 2.8 gm/cc. The non-accumulation of 0.3 percent spinel cannot be accounted for by gravitational arguments. The amount is negligible and may be due to analytical error or to the fact that the proposed parent contains 8 percent phenocrysts and may not represent a pristine liquid composition.

The most highly evolved lava, 76-15, cannot be derived from 76-9 by fractionation of megacryst phases. However, it may be derived by subtraction of phenocryst phases which would form at lower pressures, in which case approximately 50 percent of the parent composition must have crystallized in order to produce 76-15 (Fig. 4).

Phlogopite can function similarly to kaersutite in the fractionation scheme. However, no megacrysts of phlogopite were found, and we conclude that phlogopite did not play a role in the fractionation process. Nonetheless, the presence of phlogopite in the kaersutite peridotite indicates that it is an important mantle phase in which high concentrations of alkalis may reside, and it may be significant as part of the source material for alkaline mafic magmas.

Thermometry

Temperature and oxygen fugacity have been determined for one lava, 76-9, from the data of Buddington and Lindsley (1964). The apparent temperature of equilibration of the groundmass iron-titanium oxides is 1050°C at an oxygen fugacity of 10^{-10.4} bars, near the FMQ buffer.

The olivine-clinopyroxene thermometer of Powell and Powell (1974) was used to estimate the crystallization temperatures of lavas in which no ilmenite is present. Samples 76-6, 76-9, 76-23, 76-38 and 76-41 all yield temperatures of 1020°C at one bar, using average groundmass compositions of olivine and clinopyroxene. These temperatures compare favorably with the single iron-titanium oxide temperature of 1050°C for sample 76-9.

Temperatures of equilibration of orthopyroxene and clinopyroxene in xenoliths were calculated with the thermometer of Wood and Banno (1973). For the websterite (HC76-4) a temperature of 950°C was obtained, while clinopyroxenite (HC76-7) and lherzolite (PC76-6) yielded temperatures of 990°C and 910°C, respectively. If these temperatures are correct, they clearly are non-magmatic, and support the conclusion that these specific xenoliths are genetically unrelated to their host lavas.

Table 6. Chemical analyses and CIPW norms of volcanic rocks and residual glass from the San Bernardino Valley, Arizona. For key to samples, see Table 1

	76 -6	76 -9	76 -15	76 -23	76 -38	76 -41A	HC76 -2	HC76 -4	HC76 -7	PC76 -2	PC76 -6	76 -40G
SiO ₂	48.45	46.15	48.07	44.29	44.47	47.47	50.00	49.88	41.70	45.32	44.29	51.0
TiO ₂	1.73	2.20	1.84	2.63	2.57	1.98	0.66	0.50	1.16	1.73	0.01	1.38
Al ₂ O ₃	17.03	16.04	16.97	15.58	14.77	16.35	19.21	7.53	14.90	9.98	3.77	20.8
Cr ₂ O ₃	0.02	0.03	0.01	0.04	0.03	0.03	0.02	0.08	0.03	0.12	0.43	-
Fe ₂ O ₃	1.85	2.98	1.89	3.13	3.14	1.79	1.11	1.34	4.01	1.10	0.50	-
FeO	7.14	7.37	8.18	8.18	7.87	8.29	4.21	7.20	5.59	9.22	7.69	8.34
MnO	0.19	0.20	0.20	0.19	0.19	0.19	0.12	0.19	0.19	0.18	0.15	0.19
NiO	0.04	0.03	0.03	0.04	0.05	0.04	0.06	0.09	0.06	0.06	0.29	-
MgO	6.40	7.92	4.95	9.37	10.07	8.36	7.07	19.49	16.67	15.50	40.28	1.14
CaO	7.18	9.18	6.53	9.71	9.88	8.43	13.37	12.51	14.41	13.12	2.38	2.17
SrO	0.09	0.09	0.13	0.09	0.08	0.09	0.08	-	-	-	-	-
BaO	0.07	0.07	0.10	0.07	0.07	0.08	0.01	-	-	0.02	-	-
Na ₂ O	6.07	4.55	6.69	3.39	3.50	3.80	3.00	0.57	0.99	1.60	0.22	6.59
K ₂ O	2.99	1.40	3.37	1.90	1.96	2.43	0.35	0.02	0.04	0.56	0.02	9.33
P ₂ O ₅	0.38	0.41	0.77	0.26	0.26	0.14	0.12	0.04	0.07	0.15	0.05	-
H ₂ O ⁺	0.13	0.59	0.02	0.54	0.34	0.26	0.21	0.03	0.05	0.50	0.04	-
H ₂ O ⁻	0.08	0.30	0.01	0.23	0.26	0.08	0.19	0.10	0.06	0.14	0.05	-
CO ₂	-	-	-	0.08	-	0.01	0.10	0.14	0.02	0.27	0.06	-
TOTAL	99.84	99.51	99.76	99.72	99.51	99.82	99.89	99.71	99.95	99.57	100.23	100.9
Or	17.67	8.27	19.91	11.23	11.58	14.36	2.07	0.12	-	3.31	0.12	35.57
ab	13.99	17.90	13.80	9.11	7.37	14.26	24.00	4.82	-	7.05	1.86	-
an	10.39	19.21	6.32	21.68	18.80	20.38	37.92	17.93	36.10	18.40	9.24	-
lc	-	-	-	-	-	-	-	-	0.19	-	-	15.34
ne	20.25	11.16	23.19	10.60	12.05	9.69	0.75	-	4.54	3.51	-	29.82
ac	-	-	-	-	-	-	-	-	-	-	-	0.63
di-wo	9.65	10.03	9.01	10.29	12.05	8.71	11.37	17.95	12.87	18.39	0.78	4.49
di-en	5.81	6.66	4.66	6.97	8.37	5.38	7.79	13.10	10.11	12.55	0.61	1.07
di-fs	3.33	2.64	4.10	2.53	2.68	2.81	2.67	3.17	1.33	4.39	0.09	3.70
hy-en	-	-	-	-	-	-	-	21.50	-	-	15.41	-
hy-fs	-	-	-	-	-	-	-	5.20	-	-	2.17	-
ol-fo	7.10	9.16	5.37	11.47	11.71	10.82	6.88	9.76	22.01	18.26	59.07	1.24
ol-fa	4.48	4.01	5.20	4.59	4.13	6.22	2.60	2.60	3.20	7.04	9.16	4.73
cs	-	-	-	-	-	-	-	-	1.23	-	-	-
mt	2.68	4.32	2.74	4.54	4.55	2.60	1.61	1.94	5.81	1.59	0.72	1.87
cm	0.03	0.04	0.01	0.06	0.04	0.04	0.03	0.12	0.04	0.18	0.63	-
il	3.29	4.18	3.49	4.99	4.88	3.76	1.25	0.95	2.20	3.29	0.02	2.62
ap	0.09	0.97	1.82	0.62	0.62	0.33	0.28	0.09	0.17	0.36	0.12	-
cc	-	-	-	0.18	-	0.02	0.23	0.32	0.05	0.61	0.14	-
rest	0.21	0.89	0.03	0.77	0.60	0.34	0.40	0.13	0.11	0.64	0.09	-
TOTAL	99.78	99.44	99.65	99.63	99.43	99.72	99.85	99.70	99.96	99.57	100.23	101.09

G = glass analysed by microprobe; total iron reported as FeO. For calculation of Norm, same oxidation ratio as SVB76-41A assumed.

Table 7. Trace-element concentrations (in ppm) in Geronimo volcanics

	SBV76 -6	SBV76 -9	SBV76 -15	SBV76 -23	SBV76 -38	SBV76 -41A	HC76 -2	HC76 -4	HC76 -7	PC76 -2	PC76 -6
Ba	650	670	905	615	585	700	100	10	35	190	n.d.
Ce	105	70	125	65	65	70	10	5	10	15	n.d.
La	60	50	75	40	35	40	5	5	10	10	5
Nb	110	80	130	70	45	60	n.d.	5	n.d.	20	n.d.
Nd	50	40	60	35	10	30	5	n.d.	5	15	5
Pb	5	5	n.d.	n.d.	5	n.d.	n.d.	n.d.	5	n.d.	n.d.
Pr	35	30	25	n.d.	10	10	5	5	n.d.	n.d.	n.d.
Rb	65	15	70	30	30	40	5	n.d.	n.d.	5	n.d.
Sr	800	790	1105	740	710	725	690	40	90	265	5
Th	5	5	5	10	5	5	5	5	n.d.	5	n.d.
Y	30	30	30	25	25	35	10	10	15	15	n.d.
Zn	70	65	65	60	65	75	35	35	110	45	45
Zr	325	235	345	160	170	215	n.d.	15	40	70	n.d.

n.d. = not detected.

Pressure-temperature paths of basanitic liquids

In order to estimate the pressures and temperatures at which the Geronimo basalts may have been in equilibrium with enclosed megacrysts and xenoliths, the methods of Nicholls and Carmichael (1972) are employed with additional refinements given by Carmichael *et al.* (1977) and Nicholls (1977). The variation of activities of several components in a silicate melt with temperature and pressure have been calculated. (For reactions used to define these components, see Table 8.) The generalized equation utilized to calculate equilibrium pressures is

$$\ln X_i^{\text{Melt}} + \frac{\phi_i}{T} + \left[\int_1^P \bar{V}_i dP - \int_1^P V_i^0 dP \right] / RT$$

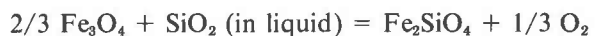
$$= \frac{G^0}{RT} + \left[\int_1^P V_s^0 dP - \int_1^P V_i^0 dP \right] / RT + \ln XS$$

where X_i^{Melt} is the mole fraction of component i , such as Fe_2SiO_4 , in the melt; ϕ_i is a parameter from regular solution theory, dependent on composition alone, which constitutes an activity coefficient for component i in the melt; XS is the activity product of the

solids appropriate to the reaction used to define the component in the melt (*e.g.*, for reaction 4, Table 8, this value would be ${}^a\text{Mg}_2\text{Si}_2\text{O}_6/{}^a\text{Mg}_2\text{SiO}_4$). The two integral expressions take into account the variation of the activity of the liquid component with pressure and the variation of the activities of solids with pressure.

The strategy employed is to take an appropriate mineral assemblage which defines a component, i , and calculate the pressure at which this assemblage would be in equilibrium with the same component in the melt as a function of temperature. A family of curves is generated, one for each reaction, that may be used to define the equilibrium states of components in the melt with the postulated solid assemblage. The intersection of these curves (ideally at a single point) then defines a region in T - P space that represents, within the precision of the method, the pressure and temperature at which the liquid was in equilibrium with the solid assemblage selected to define activities at elevated temperature and pressure. An example of the calculation using silica as a liquid component is as follows:

For sample 76-9 the reaction



may be used to define the activity of silica at surface conditions ($P = 1$ bar). A value for $\ln a_{\text{SiO}_2}$ (in melt) at 1 bar of 1.6884 is obtained from thermodynamic data supplied in Nicholls (1977). From the relationship

$$\begin{aligned} \ln a_i &= \ln X_i + \ln \gamma_i \\ &= \ln X_i + \phi/T \end{aligned}$$

one obtains for ϕ_i ,

$$\phi_i = (\ln a_i - \ln X_i)T$$

The above expression may be solved for ϕ_{SiO_2} with the groundmass temperature from iron-titanium oxides and the mole fraction of silica from a chemical analysis of the rock. The value for ϕ_{SiO_2} for lava 76-9 is -1325.27 . This method for estimating the activity of silica is only applicable to lavas containing coexisting iron-titanium oxides. However, this difficulty may be circumvented by employing the reaction



to define a_{SiO_2} . Thermodynamic data for this reaction are given in Carmichael *et al.* (1977). When this reaction is used to calculate the activity of silica for

Table 8. Reactions used to define the activities of components in silicate melts

No.	Reaction	Component
1	$\text{Fe}_2\text{SiO}_4 = \text{Fe}_2\text{SiO}_4$ Melt Olivine	Fe_2SiO_4
2	$\text{CaMgSi}_2\text{O}_6 = \text{CaMgSi}_2\text{O}_6$ Melt Clinopyroxene	$\text{CaMgSi}_2\text{O}_6$
3	$\text{NaAlSi}_3\text{O}_8 = \text{NaAlSi}_3\text{O}_8$ Melt Feldspar	$\text{NaAlSi}_3\text{O}_8$
4	$\text{Mg}_2\text{SiO}_4 + \text{SiO}_2 = \text{Mg}_2\text{Si}_2\text{O}_6$ Olivine Melt Orthopyroxene	SiO_2
5	$\text{Mg}_2\text{SiO}_4 + \text{Al}_2\text{O}_3 = 1/2 \text{Mg}_2\text{Si}_2\text{O}_6 + \text{MgAl}_2\text{O}_4$ Olivine Melt Orthopyroxene Spinel	Al_2O_3
6	$\text{NaAlSi}_3\text{O}_8 + \text{Mg}_2\text{SiO}_4 = \text{Mg}_2\text{Si}_2\text{O}_6 + \text{NaAlSi}_2\text{O}_6$ Melt Olivine Orthopyroxene Clinopyroxene	$\text{NaAlSi}_3\text{O}_8$
7	$\text{NaAlSi}_3\text{O}_8 + \text{SiO}_2 = \text{NaAlSi}_2\text{O}_6$ Melt Melt Clinopyroxene	$\text{NaAlSi}_3\text{O}_8, \text{SiO}_2$
8	$\text{CaAl}_2\text{Si}_2\text{O}_6 + \text{SiO}_2 = \text{CaAl}_2\text{Si}_2\text{O}_8$ Clinopyroxene Melt Feldspar	SiO_2
9	$3\text{CaMgSi}_2\text{O}_6 + \text{Al}_2\text{O}_3 = \text{Ca}_3\text{Al}_2\text{Si}_3\text{O}_{12}$ Clinopyroxene Melt Garnet	Al_2O_3
	+ $3/2 \text{Mg}_2\text{Si}_2\text{O}_6$ Orthopyroxene	

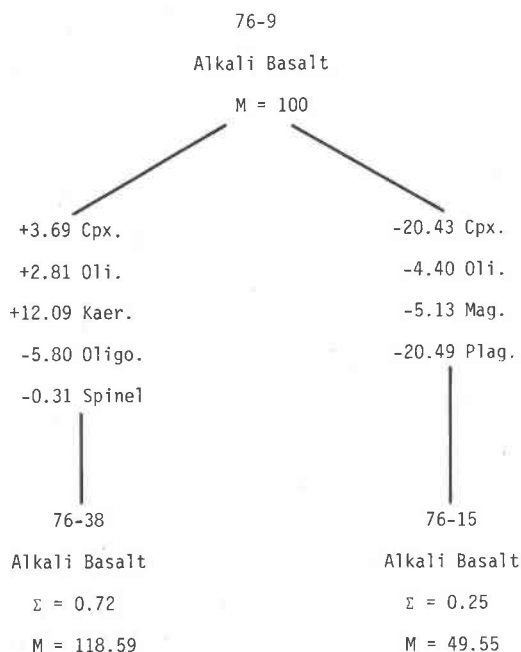


Fig. 4. Fractionation model for Geronimo Basalts as discussed in text. "M" is the mass of the new magma in each step relative to 100 units of parent magma following separation of the mineral phases. "Σ" is the sum of the squares of the residuals. Cpx. = clinopyroxene; Oli. = olivine; Kaer. = kaersutite; Oligo. = oligoclase; Mag. = magnetite; Plag. = plagioclase.

lava 76-9, a value of 1.6957 is obtained for $\ln a_{\text{SiO}_2}$, which compares quite favorably with the value of 1.6884 obtained by the previous method. The second method has been employed to estimate silica activities in lavas 76-15 and 76-38 which do not contain ilmenite.

It should be emphasized that application of the methods of reversible thermodynamics demands the assumption of equilibrium. Groundmasses of lavas are not equilibrium assemblages, the most obvious evidence being chemical inhomogeneities in most phases. We cannot assess the extent to which a groundmass deviates from equilibrium. However, the repeated and systematic pattern of chemical behavior of mineral phases in different lavas suggests that the gross deviation may not be very great. Moreover, in the lavas studied here several phases exhibit very little compositional variation. Fe-Ti oxides are homogeneous in composition; clinopyroxenes are only slightly variable in composition (Fig. 2). Olivine and plagioclase, on the other hand, exhibit substantial variability. Lacking any other alternative, we have selected average values for the compositions of these phases. This introduces an inherent error in addition to those occurring as a result of variation in standard-

state thermochemical data, activity-composition relations, and the assumption of regular solution behavior. For example, Nicholls (1977), in assessing the error introduced by variability in groundmass compositions, found that the maximum uncertainty in precision of estimates was approximately ± 7 kbar and $\pm 65^\circ\text{C}$ for the lava he tested. In applying the same criteria to our data, with olivine and albite

variations in the groundmass and equations 1 and 7 (Table 8), solutions for lherzolite source material vary by ± 7.5 kbar and $\pm 200^\circ$. This difference between our test and Nicholls' is attributable to the greater variability in olivine groundmass compositions in our lava. By applying this method to equilibrium experiments, Nicholls concluded that the accuracy of this method is approximately ± 5 kbar and $\pm 38^\circ$, due primarily to lack of precision in the thermodynamic data. Most of our results are near these limits. The results for equilibration with lherzolite are the most uncertain. Also, because lava 76-15 is not a primary magma, we anticipated that attempts to equilibrate it with lherzolite would yield large uncertainties; this proved to be true.

Three assemblages have been selected as candidates for either possible parental source rocks or residue from fractional crystallization:

- (1) Spinel lherzolite, sample PC76-6, a model residual assemblage.
- (2) Megacrysts; olivine (analysis 76-35, Table 2), clinopyroxene (from Hans Cloos Crater, Table 3), and potash oligoclase (from Cinder Hill, Fig. 3).
- (3) Phenocrysts from lavas 76-9 and 76-38.

A series of curves which give the equilibration pressure as a function of temperature for the components listed in Table 8 is shown in Figure 5 for each of these assemblages. Figure 5a gives curves for equilibration of lavas 76-9, 76-15, and 76-38 with lherzolite PC76-6. The liquid components used are fayalite (defined by reaction 1, Table 8); diopside (reaction 2); silica (reaction 4); alumina (reaction 5); and albite (reactions 6 and 7). Lava 76-9 gives intersections whose mean indicates a temperature of equilibration of $1420 \pm 100^\circ\text{C}$ at a pressure of 30 ± 8 kbar. Calculations for lava 76-38 yield similar results of $1370 \pm 70^\circ$ and 33 ± 8 kbar. If the lavas were in equilibrium with a spinel-peridotite residuum, the temperatures were 1320 to 1520°C and depths were 70 to 120 km. Similar calculations are shown for the more evolved lava 76-15 indicating equilibration at $1400 \pm 200^\circ$ and a pressure of 21 ± 13 kbar. The scatter in these calculations suggests that lava 76-15 and lherzolite were never in equilibrium, a conclusion supported by chemical and crystal fractionation arguments.

Our solutions for equilibration with spinel lherzolite fall in the experimentally-determined garnet peridotite field of O'Hara *et al.* (1971). Figure 5a includes an equilibration curve for the lavas and a hypothetical garnet peridotite assemblage (dashed line) with the mineral compositions adopted by Nich-

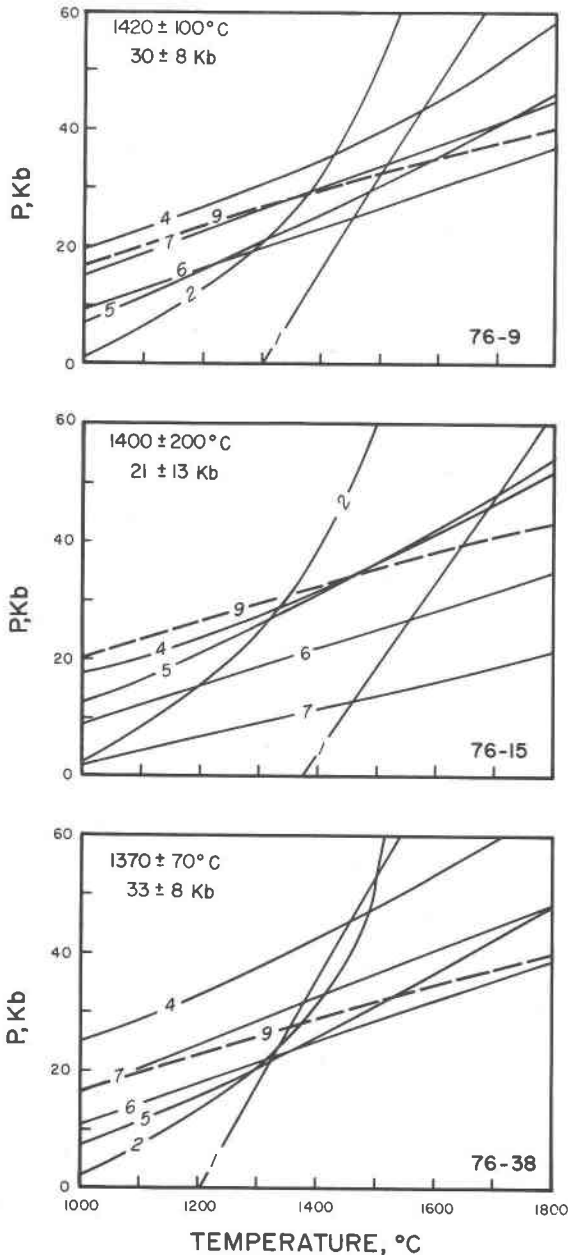


Fig. 5a. Equilibration curves between lavas 76-9, 76-15 and 76-38 and PC76-6 lherzolite. Numbers for each curve correspond to reactions in Table 8.

olls (1977). This calculation shows that the Geronimo lavas could have been in equilibrium with garnet peridotite at pressures and temperatures similar to those calculated for spinel lherzolite. Several authors have suggested that garnet is present in the source region of basanitic melts (Shimizu and Arculus, 1975; Kay and Gast, 1973). These arguments are based upon rare-earth distributions and the rare occurrence of garnet in ultramafic inclusions in some Australian basanites (Irving, 1974). We conclude that basanites are generated in the stability field of spinel lherzolite because it is the characteristic ultramafic inclusion in these lavas on a worldwide basis. Secondly, we agree with Carmichael *et al.* (1977) that source-material arguments based upon rare-earth patterns must consider the role of apatite in the fusion process. Not only is apatite strongly enriched in light rare-earth elements, but alkalic lavas contain considerable phosphorus whose concentration is positively correlated with those of the light rare earths. Finally, the starting material which O'Hara *et al.* (1971) used to define the spinel lherzolite-garnet lherzolite boundary differs in composition from the lherzolite we have employed; notably, lherzolite PC76-6 has more chrome-rich spinels. Carmichael *et al.* (1977) have suggested that chrome-rich spinels are stable to pressures at which diamonds form. If so, this allows sufficient latitude to the pressures at which spinel-bearing peridotites may be stable to accommodate our results easily.

Lherzolites may be genetically related to their host lavas, or they may be entirely accidental in their presence. Frey and Green (1974) and Stueber and Ikramuddin (1974) suggest from trace-element and isotopic evidence that many xenoliths are not cognate. However, Stull and McMillan (1973) found trace-element concentrations in some xenoliths to be consistent with cognate origin; the question remains open, although we suspect that most lherzolites are not cognate. We have used lherzolite PC76-6 simply because it occurs in one of the lavas, and we have adopted it as a model for residual mantle material in southeastern Arizona. Megacrysts, on the other hand, should be expected to provide specific genetic solutions, because they must have crystallized from silicate magmas akin to those that contain them.

Three basalts were equilibrated with the megacryst assemblage which is assumed to be common to the lavas. The results are shown in Figure 5b for reactions 1, 2, and 8, Table 8. For lava 76-9 the average solutions are very consistent, and indicate $1290 \pm 10^\circ\text{C}$ at 13 ± 0.5 kbar. Lava 76-38 indicates

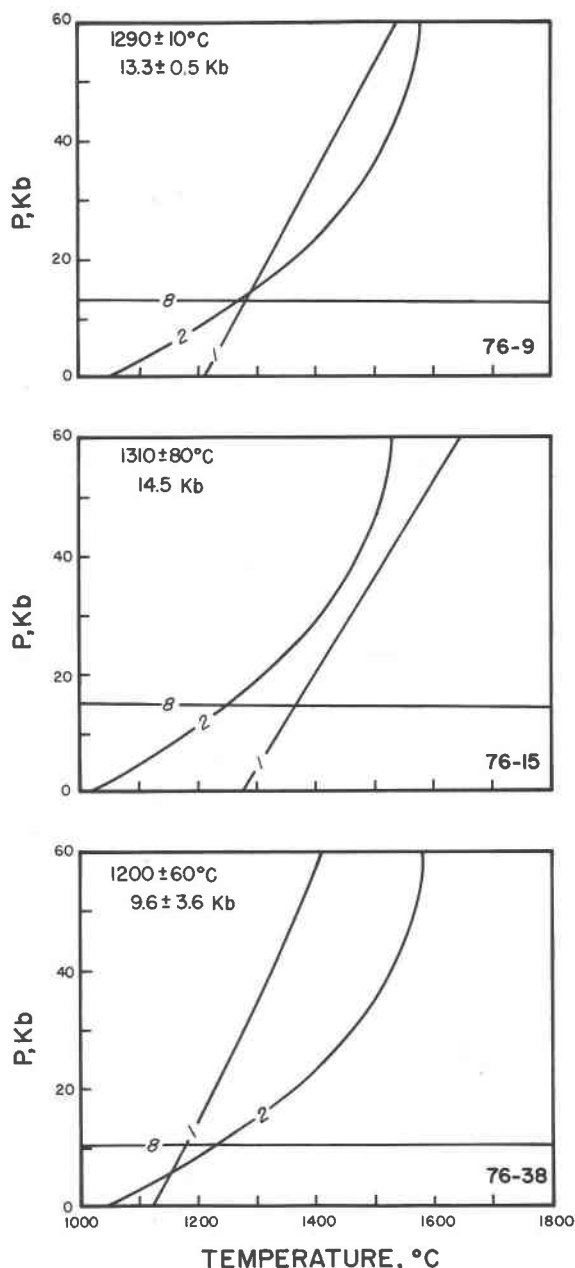


Fig. 5b. Equilibration curves between lavas 76-9, 76-15, 76-38, and megacryst assemblage.

$1200 \pm 60^\circ$ at 9.6 ± 3.6 kbar, and lava 76-15 yields $1300 \pm 80^\circ$ at 14.5 kbar. The latter solution is suspect, because crystal-fractionation models indicate that 76-15 is a derivative liquid which was not in equilibrium with the megacryst phases. Results for the megacrysts indicate that if they were ever in equilibrium with the assumed melt, temperatures were 1200 to 1300°C at depths of 30 to 46 km.

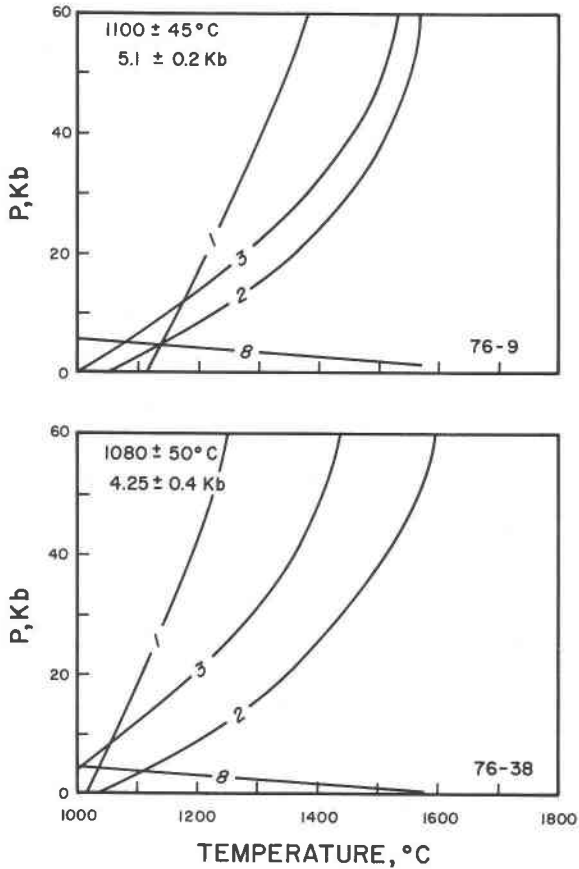


Fig. 5c. Equilibration curves between lavas 76-9 and 76-38 and phenocryst assemblage.

Figure 5c shows results of equilibrating lava 76-9 and 76-38 with their phenocrysts (lava 76-15 contains no phenocrysts). The results for lava 76-9 indicate $1100 \pm 45^\circ$ and 5.1 ± 0.2 kbar, and for lava 76-38, $1080 \pm 50^\circ$ and 4.3 ± 0.4 kbar; that is, at temperatures around 1100° and depths of 15 to 17 km in the crust. Caution should be exercised in the interpretation of these phenocryst results. Pyroxene phenocrysts have textures which could be due to the rapid disequilibrium crystallization, thus invalidating the initial assumption of equilibrium.

Equilibrium calculations by Carmichael *et al.* (1977) for a basanite, from San Quintin, Baja California, yield comparable solutions (Fig. 6). Both sets of solutions lie just slightly below an experimental liquidus for basanite (Arculus, 1975).

The same method can be applied to other xenoliths, but none warrants serious consideration. The websterite has a metamorphic texture, and although the xenolith yields reasonable solutions (1425° and 28 kbar), we consider it to be unrelated genetically to the

host lavas. Websterite and pyroxenite xenoliths yield anomalously low two-pyroxene temperatures and exhibit abundant exsolution textures. They probably represent accidental material from the mantle or lower crust. Calculations for the gabbro result in pressures in excess of the stability of its plagioclase, and again this xenolith must be considered accidental.

The several solutions for the pressure-temperature path of the lavas from source to solidification are shown in Figure 6. The pressure and temperature regime under which alkalic basalt magmas form remains poorly delineated. The region of megacryst formation, on the other hand, appears to be well constrained to the uppermost mantle.

Potential source material for basanitic magmas

In the section on barometry we demonstrated that lavas 76-38 and 76-9 could have been in equilibrium with lherzolite residue at depths of 80 to 120 km and

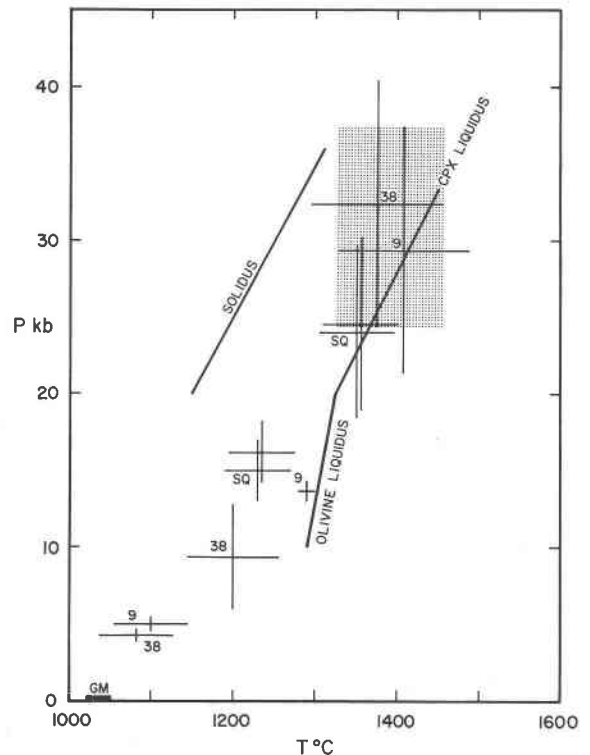


Fig. 6. Calculated equilibration temperatures and pressures for lavas 76-9 and 76-38 with lherzolite, megacrysts, and phenocrysts. Also shown are similar solutions for San Quintin basanites (SQ) (Carmichael *et al.*, 1977). The experimental solidus, olivine-liquidus and cpx-liquidus for basanite are taken from Arculus (1975). The stippled region is the area of overlap of uncertainties for the source region solutions, and GM represents the range of groundmass temperature determinations for these lavas.

temperatures of 1320 to 1520°C. A test of whether these magmas could be derived from typical mantle material may be made with numerical techniques based on the subtraction diagram method described by Bowen (1928). Potential source compositions selected were pyrolite, lherzolite, and kaersutite peridotite. Results for lava 76-9 are shown in Table 9. For a pyrolite source, 9 percent partial melting is required to produce a magma matching the composition of 76-9; it leaves a residuum whose composition is similar to that of the lherzolite (PC76-6). When lherzolite is taken as a possible source, an unrealistically small amount of partial fusion is required to arrive at a composition matching 76-9. This, and the pyrolite results, suggest that lherzolite is an unlikely parent, but may be a residuum from partial melting. Results for kaersutite peridotite indicate it represents a potential source also, but only if large degrees of partial melting were to take place.

In applying these techniques to lava 76-38, which we consider a cumulate, difficulties are immediately encountered, because it contains less silica than commonly supposed parental materials. Four potential source materials were tested (Table 10). In the cases of pyrolite and Kilborne Hole mantle (Carter, 1970) the degree of partial melting is far too small to be realistic. When more exotic kimberlitic material is

Table 9. Potential source compositions for the production of lava 76-9 by partial fusion

	76-9	Source 1	Residuum	Source 2	Residuum	Source 3	Residuum
SiO ₂	47.03	45.28	45.10	44.41	44.39	46.02	45.48
TiO ₂	2.24	0.71	0.56	0.01	0.00	1.76	1.50
Al ₂ O ₃	16.35	3.55	2.27	3.78	3.72	10.14	6.78
Cr ₂ O ₃	0.03	0.43	0.47	0.43	0.43	0.12	0.17
FeO	10.24	8.47	8.29	8.16	8.15	10.37	10.44
MnO	0.20	0.14	0.13	0.15	0.15	0.18	0.17
MgO	8.07	37.57	40.53	40.39	40.53	15.74	19.88
CaO	9.35	3.09	2.46	2.39	2.35	13.32	15.47
Na ₂ O	4.64	0.57	0.16	0.22	0.20	1.62	0.00
K ₂ O	1.43	0.13	0.00	0.02	0.01	0.57	0.11
P ₂ O ₅	0.42	0.06	0.02	0.05	0.05	0.15	0.01
% melt			9.11		0.45		35.04

Sources:

1. Pyrolite (Ringwood, 1975).
2. Lherzolite PC76-6.
3. Kaersutite peridotite PC76-2.

used, 10 percent partial melting will produce magma whose composition matches 76-38. This indicates the source region in the mantle must be silica-deficient and enriched in alkalis in comparison to more typi-

Table 10. Potential source compositions for the production of lava 76-38 by partial fusion

	76-38	Source 1	Residuum	Source 2	Residuum	Source 3	Residuum	Source 4	Residuum
SiO ₂	45.29	45.22	45.22	43.13	43.13	39.45	38.79	36.13	35.10
TiO ₂	2.62	0.24	0.22	0.33	0.33	2.60	2.60	2.35	2.32
Al ₂ O ₃	15.04	4.33	4.22	7.03	7.02	4.93	3.79	5.69	4.64
FeO	10.90	8.26	8.23	9.35	9.35	10.98	10.99	12.19	12.34
MgO	10.26	39.17	39.46	35.29	35.33	31.26	33.62	27.77	29.73
CaO	10.06	2.51	2.44	4.40	4.39	8.51	8.34	12.31	12.57
Na ₂ O	3.56	0.23	0.20	0.45	0.45	0.36	0.00	0.36	0.00
K ₂ O	2.00	0.02	0.00	0.00	0.00	1.10	1.00	2.43	2.48
P ₂ O ₅	0.26	0.02	0.02	0.01	0.01	0.81	0.87	0.77	0.83
% melt			1.01		0.15		10.10		10.10

Sources:

1. Pyrolite (Ringwood, 1975, Table 5-2, analysis 2)
2. Kilbourne hole mantle (Carter, 1970)
3. Average basaltic kimberlite (Dawson, 1967)
4. Average micaceous kimberlite (Dawson, 1967)

cal mantle material for 76-38 to be a primary magma, a condition we consider unlikely.

Summary

In the preferred model for generation of the Geronimo basalts, lava 76-9 represents a primary magma. Ten percent partial fusion of pyrolite will result in a magma whose composition matches lava 76-9. A residuum remains whose composition approximates spinel lherzolite PC76-6. This partial fusion episode took place at depths of 80 to 120 kilometers at 1320 to 1520°C. Fractionation of high-pressure megacrysts took place at a depth of 40 to 45 km and at about 1300°C, resulting in the formation of cumulate magmas represented by lavas 76-38 and 76-23. Shallow-level fractionation of phenocryst phases of olivine, clinopyroxene, magnetite, and plagioclase generated the basalts forming flows and older cones of the San Bernardino valley, whose composition is represented by lava 76-15. Eruption of large amounts of unmodified magma formed much of the valley-fill basalt and some older cones, whose composition is that of 76-9. Younger volcanism may have tapped the cumulate magma as lower levels of the magma chamber in the mantle were erupted, bringing with it the abundant megacrysts, as in the vicinity of Cinder Hill.

Acknowledgments

Financial support for this study was provided by the Research Committee of the University of Utah, the Penrose Bequest Fund of the Geological Society of America, and the Geological Research Fund of the Department of Geology and Geophysics, University of Utah. Funding for the microprobe laboratory was provided in part by the Institutional Fund of the University of Utah. The manuscript was substantially improved by the thoughtful reviews of Frank Spera and Eric Dowty.

References

- Albee, A. L. and L. Ray (1970) Correction factors for electron probe microanalysis of silicates, oxides, carbonates, phosphates and sulfates. *Anal. Chem.*, **42**, 1408-1414.
- Arculus, R. J. (1975) Melting behavior of two basanites in the range 10-35 kbar and the effect of TiO₂ on the olivine-diopside reactions at high pressures. *Carnegie Inst. Wash. Year Book*, **74**, 512-515.
- , M. A. Dungan, G. E. Lofgren and J. M. Rhodes (1977) Lherzolite inclusions and megacrysts from the Geronimo volcanic field, San Bernardino Valley, southeastern Arizona (abstr.). *Abstracts, Second International Kimberlite Conference*.
- Bacon, C. R. and I. S. E. Carmichael (1973) Stages in the *P-T* path of ascending basalt magma: an example from San Quintin, Baja California. *Contrib. Mineral. Petrol.*, **41**, 1-22.
- Bence, A. E. and A. L. Albee (1968) Empirical correction factors for the electron microanalysis of silicates and oxides. *J. Geol.*, **76**, 382-403.
- Best, M. G. (1970) Kaersutite-peridotite inclusions and kindred megacrysts in basanitic lavas, Grand Canyon, Arizona. *Contrib. Mineral. Petrol.*, **27**, 25-44.
- (1975) Amphibole-bearing cumulate inclusions, Grand Canyon, Arizona and their bearing on silica-undersaturated hydrous magmas in the upper mantle. *J. Petrol.*, **16**, 212-236.
- Binns, R. A., M. B. Duggan and J. F. G. Wilkinson (1970) High pressure megacrysts in alkaline lavas from northeastern New South Wales. *Am. J. Sci.*, **269**, 132-168.
- Bowen, N. L. (1928) *The Evolution of the Igneous Rocks*. Princeton University Press, Princeton, New Jersey.
- Brown, F. H. and I. S. E. Carmichael (1969) Quaternary volcanoes of the Lake Rudolf region: I. The basanite-tephrite series of the Korath Range. *Lithos*, **2**, 239-260.
- Buddington, A. F. and D. H. Lindsley (1964) Iron-titanium oxide minerals and synthetic equivalents. *J. Petrol.*, **5**, 310-351.
- Carmichael, I. S. E. (1967) The iron-titanium oxides of salic volcanic rocks and their associated ferromagnesian silicates. *Contrib. Mineral. Petrol.*, **14**, 36-64.
- , J. Hampel and R. N. Jack (1968) Analytical data on the U.S.G.S. standard rocks. *Chem. Geol.*, **3**, 59-64.
- , J. Nicholls, F. J. Spera, B. J. Wood and S. A. Nelson (1977) High temperature properties of silicate liquids: Applications to the equilibration and ascent of basic magma. *Trans. R. Soc. Lond.*, **286A**, 373-431.
- Carter, J. L. (1970) Mineralogy and chemistry of the Earth's upper mantle based on the partial fusion-partial crystallization model. *Bull. Geol. Soc. Am.*, **81**, 2021-2034.
- Dawson, J. B. (1967) Geochemistry and origin of kimberlite. In P. J. Wyllie, Ed., *Ultramafic and Related Rocks*, p. 269-278. Wiley, New York.
- Donaldson, C. H., T. M. Usselman, R. J. Williams and G. E. Lofgren (1975) Experimental modeling of the cooling history of Apollo 12 olivine basalts. *Proc. Lunar Sci. Conf.*, **6th**, 843-869.
- Frey, F. A. and D. H. Green (1974) The mineralogy, geochemistry and origin of lherzolite inclusions in Victorian basanites. *Geochim. Cosmochim. Acta*, **38**, 1023-1059.
- and M. Prinz (1978) Ultramafic inclusions from San Carlos, Arizona: petrologic and geochemical data bearing on their petrogenesis. *Earth Planet. Sci. Lett.*, **38**, 129-176.
- Gutmann, J. T. (1977) Textures and genesis of phenocrysts and megacrysts in basaltic lavas from the Pinacate volcanic field. *Am. J. Sci.*, **277**, 833-861.
- Hoffer, J. M. (1971) Mineralogy and petrology of the Santo Tomas-Black Mountain basalt field, Potrillo volcanics, south-central New Mexico. *Bull. Geol. Soc. Am.*, **82**, 603-612.
- and R. L. Hoffer (1973) Composition and structural state of feldspar inclusions from alkali olivine basalt, Potrillo basalt, southern New Mexico. *Bull. Geol. Soc. Am.*, **84**, 2139-2142.
- Irving, A. J. (1974) Megacrysts from the Newer Basalts and other basaltic rocks of southeastern Australia. *Bull. Geol. Soc. Am.*, **85**, 1503-1514.
- Kay, R. W. and P. W. Gast (1973) The rare earth content and origin of alkali-rich basalts. *J. Geol.*, **18**, 653-682.
- Langston, C. A. and D. V. Helmberger (1974) Interpretation of body and Rayleigh waves from NTS to Tucson. *Bull. Seis. Soc. Am.*, **64**, 1919-1929.
- Laughlin, A. W., D. G. Brookins and J. D. Causey (1972) Late Cenozoic basalts from the Bandera lava field, Valencia County, New Mexico. *Bull. Geol. Soc. Am.*, **83**, 1543-1552.
- Lofgren, G. E., C. H. Donaldson, R. J. Williams, O. Mullins, Jr. and T. M. Usselman (1974) Experimentally reproduced textures

- and mineral chemistry of Apollo 15 quartz-normative basalts. *Proc. Lunar Sci. Conf.*, 5th, 549-567.
- and T. M. Usselman (1975) Geology, petrology and crystallization of Apollo 15 quartz-normative basalts. *Proc. Lunar Sci. Conf.*, 6th, 79-99.
- Lynch, D. J. (1972) *Reconnaissance Geology of the Bernardino Volcanic Field, Cochise County, Arizona*. M.S. Thesis, University of Arizona.
- (1976) Basaltic eruptions in the Bernardino volcanic field of southeastern Arizona (abstr.). *Geol. Soc. Am. Abstracts with Programs*, 8, 604-605.
- Nicholls, J. (1977) The activities of components in natural silicate melts. In D. G. Fraser, Ed., *Thermodynamics in Geology*, p. 327-349. Reidel, Holland.
- and I. S. E. Carmichael (1972) The equilibration temperature and pressure of various lava types with spinel- and garnet-peridotite. *Am. Mineral.*, 57, 941-959.
- O'Hara, M. J., S. W. Richardson and G. Wilson (1971) Garnet-peridotite stability and occurrence in crust and mantle. *Contrib. Mineral. Petrol.*, 32, 48-68.
- Powell, M. and R. Powell (1974) An olivine-clinopyroxene geothermometer. *Contrib. Mineral. Petrol.*, 48, 249-263.
- Ringwood, A. E. (1975) *Composition and Petrology of the Earth's Mantle*. McGraw-Hill, New York.
- Roy, R. F., D. D. Blackwell and E. R. Decker (1972) Continental heat flow. In E. C. Robertson, Ed., *The Nature of the Solid Earth*, p. 506-543. McGraw-Hill, New York.
- Shimizu, N. and R. J. Arculus (1975) Rare earth element concentrations in a suite of basanitoids and alkali olivine basalts from Granada, Lesser Antilles. *Contrib. Mineral. Petrol.*, 50, 231-240.
- Smith, A. L. and I. S. E. Carmichael (1969) Quaternary trachybasalts from southeastern California. *Am. Mineral.*, 54, 909-923.
- Stormer, J. C., Jr. (1973) Calcium zoning in olivine and its relationship to silica activity and pressure. *Geochim. Cosmochim. Acta*, 37, 1815-1821.
- and J. Nicholls (1978) XLFRAC: A program for the interactive testing of magmatic differentiation models. *Computers and Geosciences*, 4, 143-159.
- Stueber, A. M. and M. Ikramuddin (1974) Rubidium, strontium and the isotopic composition of strontium in ultramafic nodule minerals and host basalts. *Geochim. Cosmochim. Acta*, 38, 207-216.
- Stull, R. J. and K. McMillan (1973) Origin of lherzolite inclusions in the Malapai Hill basalt, Joshua Tree National Monument, California. *Bull. Geol. Soc. Am.*, 84, 2343-2350.
- Thornton, C. P. and O. F. Tuttle (1960) Chemistry of igneous rocks: pt. I. Differentiation index. *Am. J. Sci.*, 258, 664-684.
- Wilkinson, J. F. G. (1975) An Al-spinel ultramafic inclusion suite and high pressure megacrysts in an analcinite and their bearing on basaltic magma fractionation at elevated pressures. *Contrib. Mineral. Petrol.*, 53, 71-104.
- Wood, B. J. and S. Banno (1973) Garnet-orthopyroxene and orthopyroxene-clinopyroxene relationships in simple and complex systems. *Contrib. Mineral. Petrol.*, 42, 109-124.

*Manuscript received, June 6, 1978;
accepted for publication, October 11, 1978.*